

A Page-Hinkley Based Method for HFOs Detection in Epileptic Depth-EEG

Nisrine Jrad^{1,2}, Amar Kachenoura^{1,2}, Anca Nica^{1,2,3}, Isabelle Merlet^{1,2}, Fabrice Wendling^{1,2}

¹INSERM, U1099, Rennes, F-35000, France, ²Université de Rennes 1, LTSI, Rennes, F-35000, France,

³Unité d'Epileptologie, Service de Neurologie, CHU, Rennes, F-35000, France.

Abstract—Interictal High Frequency Oscillations, (HFOs [30-600 Hz]), recorded from intracerebral electroencephalo-graphy (iEEG) in epileptic brain, showed to be potential biomarkers of epilepsy. Hence, their automatic detection has become a subject of high interest. So far, all detection algorithms consisted of comparing HFOs energy, computed in bands of interest, to a threshold. In this paper, a sequential technique was investigated. Detection was based on a variant of the Cumulative Sum (CUSUM) test, the so-called Page-Hinkley algorithm showing optimal results for detecting abrupt changes in the mean of a normal random signal. Experiments on simulated and real datasets showed the good performance of the method in terms of sensitivity and false detection rate. Compared to the classical thresholding, Page-Hinkley showed better performance.

Keywords—Abrupt change, Page-Hinkley algorithm, Cumulative Sum test, Gabor Transform, intracerebral electroencephalo-graphy, epilepsy, interictal High Frequency Oscillations.

I. INTRODUCTION

Digital recording systems with high sampling rates revealed High Frequency Oscillations (HFOs [30-600 Hz]) in intracerebral ElectroEncephaloGraphy (iEEG). Studies of pathological HFOs in epileptic brains proved the correlation of HFOs with the epileptogenic zone [1]. Interestingly, interictal and ictal HFOs showed similar spectral [2] and spatial features [3], making their recordings independent of seizures. Moreover, interictal HFOs were correlated with good post-surgical outcomes more than ictal patterns or Interictal Epileptic Spikes (IES) [4]. In this context, the accurate detection of HFOs is to be foremost. However, physiological properties of HFOs make their detection a non-trivial task. HFOs are non-stationary transient events of low amplitude. Recordings are usually contaminated by artefacts (IES, sharp waves, muscle, etc.) yielding false detections. Moreover, HFOs have a wide diversity. They are divided into four classes according to their frequency extent; low-gamma [5] (γ [30-80 Hz]), high-gamma [6] ($H\gamma$ [80-120 Hz]), Ripples (Rs [120-250 Hz]) and Fast Ripples (FRs [250-600 Hz]) [7].

So far, all methods have used energy thresholding to detect HFOs. Indeed, an energy distribution was computed in the spectral domain (HFOs band of interest). This energy was compared to a threshold in order to detect HFOs occurrence. The main objective of this work is to study the efficiency of a sequential abrupt change detection method, Page-Hinkley [8], in HFOs detection. To this end, signal was decomposed, using Gabor atoms [9], into its contributions in the human physiological frequency bands. Energy on the HFOs bands was

computed. Page-Hinkley algorithm was applied to detect the average energy changes induced by HFOs. Results on simulated and real data sets were compared to the thresholding technique. Page-Hinkley based detector showed competitive performance in terms of sensitivity and false detection rate.

II. STATE OF THE ART

Initial detection of HFOs was visual. Results were quite subjective, marginally consistent and non-reproducible. Consequently, automated algorithms were investigated. iEEGs were first preprocessed by band pass filtering the signal, in a frequency band of interest, using finite or infinite impulse response or first order backward differencing filters. The frequency band was set according to the physiological bands: Rs and FRs bands in [7] and γ band in [5]. An energy measure was then computed, based on the preprocessed signal, and a threshold was applied to detect HFOs. Early methods studied HFOs in the time domain. Different energy norms were computed on a sliding window, like L2-norm in [7], L1-norm in [5] or Hilbert envelope in [10]. Amplitude and duration thresholds were used to characterize HFOs. Recently, the time-frequency space was parameterized and thresholding technique was also used to detect the occurrence of HFOs [11]. To sum up, all detection techniques compared energy to a threshold.

In this paper, a sequential analysis, Page-Hinkley was investigated [8]. Page-Hinkley is a variant of the CUMulative SUM (CUSUM) test. It has optimal properties detecting changes in the average of a normal process [12]. In the context of iEEG analysis, Page-Hinkley was proposed as a segmentation tool of seizure signals [13]. It showed competitive results, compared to thresholding, detecting clonic spike discharges and low amplitude tonic rapid discharges. Analogously, it was successfully exploited to detect rapid discharges, in iEEG signals, during transition to seizure [14]. It was also used in [15] to detect interictal epileptic spikes. To the best of authors' knowledge, this type of approach was never proposed in the context of HFOs so far.

III. MATERIALS

Pseudo-real signals and human iEEG signals were considered to evaluate the efficiency of the proposed method.

A. Human Signals

iEEG signals from five pharmaco-resistant patients were recorded in the Neurology department of the University Hospital of Rennes in France. A 256-channel Brain Quick® (Micromed, Italy) acquisition system, with a sampling rate of

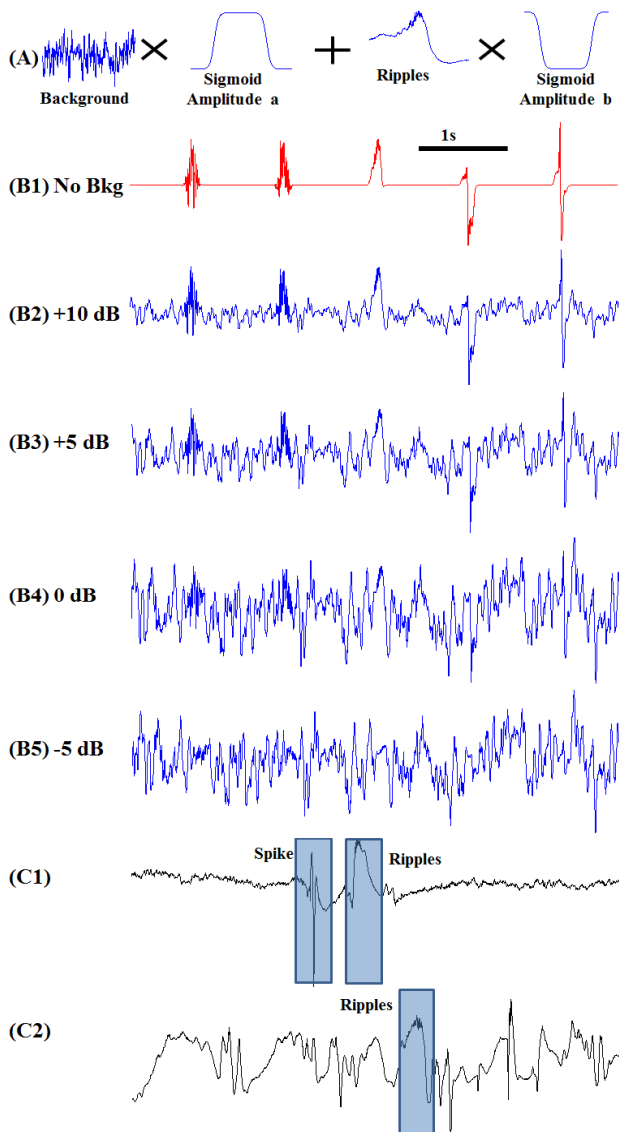


Fig. 1. Simulated and real data. (A) Events extracted from real iEEG were inserted in the neuronal activity. Various background levels were used to set Event to Background Ratios (EBR). (B1) to (B5) are examples of 5.5 s simulated iEEG including γ , $H\gamma$, Rs , FRs and IES at 0.75 s, 1.75 s, 2.75 s, 3.75 s and 4.75 s for different EBR: (B1) No background, (B2) EBR = 10 dB, (B3) EBR = 5 dB, (B4) EBR = 0 dB and (B5) EBR = -5 dB. (C1) and (C2) are two iEEGs signals from different patients.

2048 Hz, was used to record iEEG. No hardware filter was applied in the acquisition procedure, except the high-pass filter with 0.1 Hz as a cut-off frequency. It removes the offset of the baseline. Two reviewers did the manual annotation independently. Visually detected events were labeled as γ , $H\gamma$, Rs , FRs or Interictal Epileptic Spikes (IES). IES were considered because they often lead to false detection. Around 2200 minutes were reviewed. A total number of 6903 events were visually labeled. Four categories were visually detected and labeled as γ (1724 events), $H\gamma$ (1085 events), Rs (2019 events) and FRs (1476 events). IES (599 events) were also identified.

B. Simulated signals

To compare Page-Hinkley algorithm to the thresholding technique, pseudo-real signals were simulated. Background activities, imitating human signals, were generated using a neuronal model as proposed in [16]. Transient events (γ , $H\gamma$, Rs FRs and IES), detected from patients were inserted into background. To avoid sharp transitions between events and background, weighted sigmoid functions were used. Sigmoid amplitudes controlled the Events to Background Ratio (EBR). Signals of thirty minutes were simulated with an average of fifteen events (three for each kind of HFOs) per minute and an EBR of -5 to +10 dB with a step of 5. Examples are illustrated in Figure 1. A segment of 5.5 s simulated signal is shown with γ , $H\gamma$, Rs FRs and IES inserted at $t = 0.75, 1.75, 2.75, 3.75$ and 4.75 s. Events are hardly discriminated from background for negative EBR. A 5.5 s segment of two patients recordings are also illustrated in C1-C2. Simulated signals above 0 dB look very representative of the real ones.

IV. METHODS

In the sequel, both Page-Hinkley and thresholding algorithms are presented.

A. Problem statement

Let us denote by $s(t) \in \mathbb{R}^S$ the signal recorded on one iEEG channel with S the total number of samples. This signal includes background activity in which transient events appear randomly. Transient events regroup all kinds of HFOs (γ , $H\gamma$, Rs , and FRs) and artefact, such as IES (ART/IES). The objective of this paper is to propose a method to detect HFOs that is more accurate than the classical thresholding one.

B. HFOs detection methods

Raw signals were decomposed, using Gabor function [9], into their contributions in the HFOs bands. The Gabor atoms were chosen optimally regarding the time-frequency uncertainty principle (see [9] and our previous works [17, 18] for more details). Gabor function is defined as a Gaussian envelope modulated by complex sinusoids:

$$g(t; f_0, \sigma) = \frac{1}{\sqrt{2\pi}\sigma} e^{-\frac{t^2}{2\sigma^2}} e^{j2\pi f_0 t} \quad (1)$$

The frequency f_0 centers the modulated Gaussian. The scale parameter σ sets its sharpness and defines the extent of Gabor function since it determines its rate of convergence toward zero. A set of Gabor functions, with spectral representation covering high frequencies (γ , $H\gamma$, Rs , FRs) were selected by tuning $f_0^{(j)}$ and $\sigma^{(j)}$. The Gabor Transform of $s(t)$ is:

$$c(t; f_0, \sigma) = s(t) * g(t; f_0, \sigma) = \sum_{\tau=-\infty}^{+\infty} s(\tau) g(t-\tau; f_0, \sigma) \quad (2)$$

The local energy, at frequency band j was, then, computed over a sliding rectangular window of width N , w_N . For each of the HFOs bands, the moving average energy was given by:

$$\varepsilon^{(j)}(t) = \sqrt{\frac{1}{N} \sum_{\tau} (c(\tau; f_0^{(j)}, \sigma^{(j)}))^2 w(\tau-t)} \quad (3)$$

The total energy was computed as the sum of energies in the γ , H γ , Rs and FRs bands:

$$\varepsilon^{(Tot)}(t) = \sum_{j=\gamma}^{\text{FRs}} \varepsilon^{(j)}(t) \quad (4)$$

This energy was then analyzed to detect HFOs occurrence.

The Page-Hinkley algorithm: The detection of HFOs can be viewed as hypotheses testing problem on the piecewise stationary sequence energy $\varepsilon^{(Tot)}(t)$. Indeed, assume that the sequence $\varepsilon^{(Tot)}(t)$, $t \in \{1, \dots, T\}$, $T < S$ follows the model:

$$\varepsilon^{(Tot)}(t) = \mu(t) + \phi^{(Tot)}(t) \quad (5)$$

where $\mu(t)$ is the mean of $\varepsilon^{(Tot)}(t)$ at sample t and $\phi^{(Tot)}(t)$, $t \in \{1, \dots, T\}$ is a sequence with T mutually independent random variables of zero mean. The occurrences of HFOs corresponds to abrupt changes in the average of $\varepsilon^{(Tot)}(t)$ and the decision rule, at sample t , can be calculated according to the two following hypothesis:

$$\begin{aligned} H_0 : \mu(t) &= \mu_0 \text{ for } t = 1, \dots, T \\ H_1 : \mu(t) &= \begin{cases} \mu_0 & \text{for } t = 1, \dots, (t_{\text{change}} - 1) \\ \mu_1 & \text{for } t = t_{\text{change}}, \dots, T \end{cases} \end{aligned} \quad (6)$$

where μ_0 and μ_1 ($\mu_1 > \mu_0$) represent the mean values before and after the unknown rupture sample change t_{change} , corresponding to the HFOs onset. Under the assumption that $\phi^{(Tot)}(t)$, $t \in \{1, \dots, T\}$ is a Gaussian random process, the log-likelihood ratio can be reduced to:

$$\Lambda(t_{\text{change}}) = \frac{\delta}{\sigma^2} \sum_{t=t_{\text{change}}}^T \left(\varepsilon^{(Tot)}(t) - \mu_0 - \frac{\delta}{2} \right) = \frac{\delta}{\sigma^2} \Gamma_{t_{\text{change}}}^T(\mu_0, \delta) \quad (7)$$

where σ^2 represents the variance of the sequence $\phi^{(Tot)}(t)$ and $\delta = \mu_1 - \mu_0$. Then maximizing the log-likelihood ratio is equivalent to maximizing $\Gamma_{t_{\text{change}}}^T(\mu_0, \delta)$ in order to estimate the sample of rupture:

$$\hat{t}_{\text{change}} = \arg \max_{2 \leq t_{\text{change}} \leq T} \left(\Gamma_{t_{\text{change}}}^T(\mu_0, \delta) \right) \quad (8)$$

This implies that the average jump detection test is written as:

$$\begin{aligned} g_T &= \max_{2 \leq t_{\text{change}} \leq T} \left(\Gamma_{t_{\text{change}}}^T(\mu_0, \delta) \right) = \Gamma_1^T(\mu_0, \delta) - \min_{2 \leq t \leq t_{\text{change}}} \left(\Gamma_1^t(\mu_0, \delta) \right) > \lambda_p \\ &\quad H_1 \\ &\quad H_0 \end{aligned} \quad (9)$$

By replacing the index T with the current index t_c , we obtained the well-known Page-Hinkley test and the detection of the average jump (detection of HFOs in our context) holds when:

$$g_{t_c} = \Gamma_{t_c}^{t_c}(\mu_0, \delta) - \min_{2 \leq t \leq t_c} \left(\Gamma_1^t(\mu_0, \delta) \right) > \lambda_p \quad (10)$$

The estimate of the sample of rupture \hat{t}_{change} is provided by the last index for which the minimum value of $\Gamma_1^t(\mu_0, \delta)$ is reached. In our case the expected mean jump δ is unknown and the Page-Hinkley test can be reformulated as follows:

1. Define a minimum jump δ_p .
2. Calculate the cumulative sum
- $m(0) = 0$ and $m(t_c) = \sum_{t=1}^{t_c} \left(\varepsilon^{(Tot)}(t) - \mu_0 - \frac{\delta_p}{2} \right)$.
3. Calculate the minimum evidence $m_{\min} = \min_{2 \leq t \leq t_c} m(t)$.
4. The estimated sample of detection \hat{t}_{change} is obtained when $m(t_c) - m_{\min} > \lambda_p$ and the corresponding t_c is called the alarm time.
5. After each detection, the algorithm is frozen during a few samples (generally the average duration of FRs since they are the shortest HFOs). Then, the algorithm is re-initialized (go to step 2).

Obviously, results depend on the magnitude δ_p and the detection threshold λ_p . These parameters are used to adjust the tradeoff between sensitivity and False Detection Rate (FDR). The magnitude stands δ_p for the tolerated changes that will not raise an alarm. The detection threshold λ_p tunes the false alarm rate. Larger thresholds entail fewer false alarms while increasing miss detections.

Page-Hinkley algorithm was compared to the typical thresholding strategy classically used to detect HFOs [7]. Usually, the total energy (4) was compared to a threshold λ_T set as a percentile of the cumulative distribution function of the total energy computed over the signal. Successive energy segments with amplitudes above threshold λ_T and longer than 6.5 ms in duration were detected and delineated by an onset and an offset boundary limit markers.

The behavior of both algorithms is exemplified in Figure 2. It shows a segment of an iEEG signal with two HFOs: Rs followed by FRs of higher amplitude. The spectrogram illustrates the big difference in energy of both HFOs. Changes in energy, computed in HFOs band using Gabor Transform, was exploited to detect time occurrence of HFOs. Thresholding algorithm showed that, for optimal value of λ_T , the first HFOs were missed. Page-Hinkley algorithm, applied with its optimal parameters, led to the detection of both HFOs (red arrows of 2.D). A magnified view of the cumulative sum illustrated how it reached a minimal value, m_{\min} , then increased when Rs occurred. Detection was declared when $m(t) - m_{\min}$ reached the threshold λ_p and given by \hat{t}_{change} .

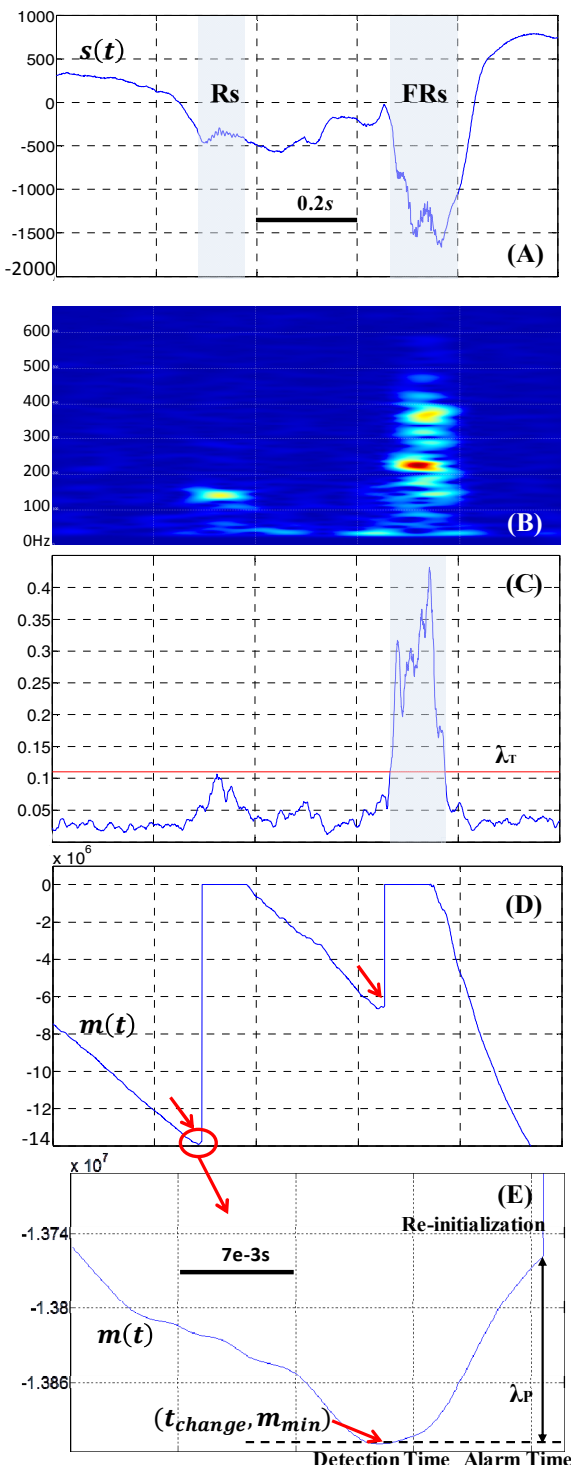


Figure 2: Representative behavior of both methods when applied to an iEEG signal. (A) Raw signal presenting Rs at 0.3s and FRs at 0.7s. (B) Spectrogram of Rs showing a high energy around 120 Hz and that of FRs with high energy spreading between 250 and 400 Hz (C) Comparison of the total energy (4), computed in τ , $H\tau$, Rs and FRs bands, to the threshold, leads to one detection (highlighted). (D) Page-Hinkley algorithm performed on the total energy: the cumulative sum monotonically decreases when there is no change in the signal; it reaches a local minimum when HFOs appear (detection time given by the two red arrows). (E) Magnified view of the cumulative sum when Rs start. A significant change occurs at alarm time, when the increase of the cumulative sum from the last local minimum (providing the detection time) is greater than threshold λ_p .

TABLE I

Table I: Performance on simulated and real data. For both Page-Hinkley and thresholding algorithms: mean (standard deviation) of Sensitivity and FDR.

| | Page-Hinkley | | Threshold | | |
|-------|---------------|---------------|---------------|---------------|-----|
| | dB | Sensitivity | FDR | Sensitivity | FDR |
| +10 | 0.986 (0.009) | 0.219 (0.021) | 0.873 (0.010) | 0.236 (0.023) | |
| +5 | 0.924 (0.026) | 0.203 (0.014) | 0.786 (0.087) | 0.196 (0.024) | |
| 0 | 0.747 (0.085) | 0.254 (0.055) | 0.688 (0.048) | 0.226 (0.055) | |
| -5 | 0.430 (0.014) | 0.233 (0.023) | 0.404 (0.018) | 0.249 (0.025) | |
| Human | 0.913 (0.112) | 0.431 (0.226) | 0.899 (0.111) | 0.535 (0.247) | |

V. RESULTS AND DISCUSSION

A. Experiments

Two experiments were considered to compare detection algorithms. The first was conducted on simulated data sets described above. The percentage of ART/IES was set to 20% of inserted events on average. The objective of considering these simulated sets was to assess and compare both methods when the occurrence time and the category of EoIs were known a priori (ground truth). Another goal was to evaluate the robustness of the detection methods to EBR. The second experiment was conducted on human recordings to measure the efficiency of the method on real depth-EEG signals. In this case, the clinical reviews were considered as the ground truth. For both simulated and real data, iEEG signals were divided into a training set (70% of iEEG) and a testing set (30% of iEEG). The training set was used to select the parameters on a ROC curve (δ_p, λ_p for Page-Hinkley algorithm and λ_T for thresholding algorithm). The test set was used to compute sensitivity and FDR on a blind set.

B. Results and discussions

Mean and standard deviation of sensitivity and FDR were reported in Table I, for Page-Hinkley and thresholding algorithms. Results on simulated data showed that, for EBRs close to real iEEG ones (above 0 dB), Page-Hinkley performance were competitive. Indeed, sensitivities were greater than 0.924 (0.026) with FDRs equal to the amount of ART/IES inserted. When EBR was low, sensitivities decreased to reach 0.430 (0.014) at its lowest value. Besides, FDRs increased. We can deduce that background activities introduce false detections together with the inserted ART/IES. These results seem coherent with visual detections. Indeed, for low EBR (0 and -5 dB), events were visually undetectable and the amplitude of background activity was prominent.

When comparing Page-Hinkley to thresholding, we notice that, for all EBRs, Page-Hinkley sensitivities were higher than thresholding ones with smaller FDRs. As an example, sensitivities/FDRs obtained when using Page-Hinkley versus thresholding for EBR = 5 dB were 0.986 (0.009) vs 0.873 (0.010) and 0.219 (0.021) vs 0.236 (0.023). Moreover, standard deviations were smaller for Page-Hinkley algorithm than for thresholding. This means that Page-Hinkley performance were more consistent than thresholding ones. Results on real data

showed that Page-Hinkley algorithm decreases FDRs with a slight increase in sensitivity as compared to thresholding results. Sensitivities were around 0.913 (0.112), which is equal to sensitivities of simulated data with high EBR. However, FDRs computed on real iEEGs were higher than FDRs computed on simulated data. This clearly reflected that iEEG signals were highly contaminated with artefacts and revealed the need of classifying the detected events like we did in [17]. To sum up, Page-Hinkley showed better performance than thresholding on both real data, and simulated data with EBR close to real iEEG ones. Actually, we zoomed in some performance computed on iEEGs signals with high EBR. We found that for a sensitivity of 1, computed on 25 minutes of signals presenting mainly Rs oscillations together with IES, FDRs were of 0.384 for Page-Hinkley and 0.529 for thresholding. Finally, to compare Page-Hinkley performance to thresholding ones, we can cite results of a comparative study [19]. This latter reported sensitivities ranging from 87.6 (21) and 97.6 (10) and their corresponding FDRs of 70.9 (26) and 75.7 (24).

As for complexity, both algorithms are easy to implement and tune. Although Page-Hinkley efficiency depends on two parameters, while thresholding performance depends on only one parameter, its optimality was theoretically proved in a normal random process [12] and experimentally illustrated in this study. Moreover, previous experimental studies supported this statement. For instance, authors of [20] showed that Page-Hinkley had very competitive performance, in terms of sensitivity and specificity, when used to detect epileptic spikes. Similarly, results of a comparative seizure detection study [13] corroborated these findings.

VI. CONCLUSION

Automatic detection methods of interictal High Frequency Oscillations (HFOs), as a reliable biomarker of epilepsy, have emerged. Thresholding energy was classically and so far, the unique method used to detect HFOs. In this work Page-Hinkley algorithm was applied on energy computed using Gabor Transform. Page-Hinkley algorithm detected changes on the energy average to declare occurrences of HFOs. Page-Hinkley detector was compared to the thresholding one. Results on simulated and real data showed that Page-Hinkley algorithm was better than thresholding.

ACKNOWLEDGMENT

This research is supported by ANR, project FORCE, ANR-13-TECS-0013

REFERENCES

- [1] J. Jacobs, P. LeVan, R. Chander, J. Hall, F. Dubeau, and J. Gotman, "Interictal high-frequency oscillations (80-500 Hz) are an indicator of seizure onset areas independent of spikes in the human epileptic brain," *Epilepsia*, vol. 49, no. 11, pp. 1893-907, Nov 2008.
- [2] G. A. Worrell, L. Parish, S. D. Cranstoun, R. Jonas, G. Baltuch, and B. Litt, "High-frequency oscillations and seizure generation in neocortical epilepsy," *Brain*, vol. 127, no. Pt 7, pp. 1496-506, Jul 2004.
- [3] M. Zijlmans, J. Jacobs, Y. U. Kahn, R. Zelmann, F. Dubeau, and J. Gotman, "Ictal and interictal high frequency oscillations in patients with focal epilepsy," *Clin Neurophysiol*, vol. 122, no. 4, pp. 664-71, Apr 2011.
- [4] J. Jacobs *et al.*, "High-frequency electroencephalographic oscillations correlate with outcome of epilepsy surgery," *Ann Neurol*, vol. 67, no. 2, pp. 209-20, Feb 2010.
- [5] A. B. Gardner, G. A. Worrell, E. Marsh, D. Dlugos, and B. Litt, "Human and automated detection of high-frequency oscillations in clinical intracranial EEG recordings," *Clin Neurophysiol*, vol. 118, no. 5, pp. 1134-43, May 2007.
- [6] S.-C. Park, S. K. Lee, H. Che, and C. K. Chung, "Ictal high-gamma oscillation (60-99 Hz) in intracranial electroencephalography and postoperative seizure outcome in neocortical epilepsy," *Clinical Neurophysiology*, vol. 123, no. 6, pp. 1100-1110, 6// 2012.
- [7] R. J. Staba, C. L. Wilson, A. Bragin, I. Fried, and J. Engel, Jr., "Quantitative analysis of high-frequency oscillations (80-500 Hz) recorded in human epileptic hippocampus and entorhinal cortex," *J Neurophysiol*, vol. 88, no. 4, pp. 1743-52, Oct 2002.
- [8] D. V. Hinkley, "Inference about the change-point from cumulative sum tests," *Biometrika*, vol. 58, no. 3, pp. 509-523, 1971.
- [9] D. Gabor, "Theory of Communication," *IEE, Journal* vol. 93, no. 26, 1946.
- [10] B. Crepon *et al.*, "Mapping interictal oscillations greater than 200 Hz recorded with intracranial macroelectrodes in human epilepsy," *Brain*, vol. 133, no. Pt 1, pp. 33-45, Jan 2010.
- [11] S. Chaibi, T. Lajnef, Z. Sakka, M. Samet, and A. Kachouri, "A comparison of methods for detection of high frequency oscillations (HFOs) in human intacerbral EEG recordings," *American Journal of Signal Processing*, vol. 3, no. 2, pp. 25-34, 2013.
- [12] M. Basseville and I. V. Nikiforov, *Detection of abrupt changes: theory and application*. Prentice Hall Englewood Cliffs, 1993.
- [13] F. Wendling, G. Carraut, and J. Badier, "Segmentation of depth-EEG seizure signals: method based on a physiological parameter and comparative study," *Annals of biomedical engineering*, vol. 25, no. 6, pp. 1026-1039, 1997.
- [14] F. Bartolomei, P. Chauvel, and F. Wendling, "Epileptogenicity of brain structures in human temporal lobe epilepsy: a quantified study from intracerebral EEG," *Brain*, vol. 131, no. Pt 7, pp. 1818-30, Jul 2008.
- [15] M. Gavaret *et al.*, "Source localization of scalp-EEG interictal spikes in posterior cortex epilepsies investigated by HR-EEG and SEEG," *Epilepsia*, vol. 50, no. 2, pp. 276-289, 2009.
- [16] F. Wendling, A. Hernandez, J.-J. Bellanger, P. Chauvel, and F. Bartolomei, "Interictal to ictal transition in human temporal lobe epilepsy: insights from a computational model of intracerebral EEG," *Journal of Clinical Neurophysiology*, vol. 22, no. 5, p. 343, 2005.
- [17] N. Jrad *et al.*, "Automatic detection and classification of High Frequency Oscillations in depth-EEG signals," *IEEE Transactions on Biomedical Engineering*, vol. PP, no. 99, pp. 1-1, 2016.
- [18] N. Jrad, A. Kachenoura, I. Merlet, and F. Wendling, "Gabor transform for interictal high frequency oscillations classification," in *2015 International Conference on Advances in Biomedical Engineering (ICABME)*, 2015, pp. 127-130.
- [19] R. Zelmann, F. Mari, J. Jacobs, M. Zijlmans, F. Dubeau, and J. Gotman, "A comparison between detectors of high frequency oscillations," *Clin Neurophysiol*, vol. 123, no. 1, pp. 106-16, Jan 2012.
- [20] O. Khouma, M. L. Ndiaye, S. M. Farsi, J.-j. Montois, I. Diop, and B. Diouf, "Comparative methods of spike detection in epilepsy," in *Science and Information Conference (SAI)*, 2015, 2015, pp. 749-755: IEEE.